

DYNAMIC TIDAL ALIGNMENT OF CLUSTER GALAXIES

M. J. PEREIRA AND J. R. KUHN

Institute for Astronomy, University of Hawaii, Honolulu-HI-96822

Draft version November 19, 2018

ABSTRACT

We investigate the role of parametric tidal interactions between cluster galaxies and the cluster potential by considering galaxy and cluster dynamical properties and drawing an analogy between these systems and the Milky Way-dSph system. We suggest that some cluster galaxies are indeed undergoing resonant excitation and argue that this will cause a tendency for alignment of the galaxies' long axis along the radial direction (towards the cluster center). We look for this signature in a sample of 70 x-ray selected clusters observed by the Sloan Digital Sky Survey, and find robust statistical evidence for the existence of a radial alignment mechanism.

Subject headings: galaxies: elliptical — Galaxy: evolution — galaxies: kinematics and dynamics

1. INTRODUCTION

The question of whether there are large scale systematic galaxy alignments, and their implications for galaxy formation, goes back many years. Hawley and Peebles (1975) reviewed some of the early speculation about how fossil eddy turbulence or primeval magnetic fields might be a cause for such anisotropy. Another mechanism, the tidal influence of a galaxy cluster's gravitational field, is an obvious possibility for aligning cluster galaxies but the physics of this process does not seem to have been elucidated. A particularly interesting question is whether galaxy alignment is a feature of the initial conditions of cluster formation, which might then decay with galaxy-cluster and galaxy-galaxy interactions, or whether it is a dynamical effect that grows with galaxy and cluster evolution.

We argue that the dynamical properties of cluster elliptical galaxies are, in some ways, similar to local group dwarf spheroidals (dSph). In that case, by accounting for the time dependence of the Milky Way (MW) tides, the interaction cross-section of a dSph with the MW gravitational field can be significantly larger than "static" estimates. We show here that coherent effects, analogous to planetary rotation tidal locking, can affect the orientation of galaxies in a cluster. The dynamically magnified cluster tidal interaction can also play an important role in the formation and evolution of cluster elliptical galaxies. Our proposal here refines the "galaxy harassment" cluster evolution scenario (cf. Moore et al. 1996) and the numerically described effects of, for example, Muccione and Ciotti (2004).

Even before sensitive largescale photographic surveys existed, Brown (1938) suggested that galaxy orientations are not isotropic. Hawley and Peebles (1975) may have been the first to analyze a large modern galaxy database, and they found statistically weak evidence that Coma cluster galaxies are preferentially oriented toward the cluster center. Others have also found marginal evidence of radial galaxy alignment in the Coma cluster (Thompson 1976; Djorgovski 1983) and, on larger scales, alignment with the cluster axis or with respect to nearby clusters (i.e. Binggeli 1982; Lambas, Groth, and Peebles 1988; Chambers, Melott, Miller 2002; Plionis et al. 2003). Galaxy cluster data generally support the view

that clusters and their brightest galaxies do tend to align (cf Plionis et al. 2003) although alignment of a significant population of cluster galaxies with the cluster axis or toward the cluster center is not established (i.e. Kindl 1987; Fong, Stevenson, Shanks 1990; van Kampen and Rhee 1990; Trevese, Cirimele, and Flin 1992; Abell, Corwin, and Olowin 1989).

2. PARAMETRIC TIDAL EFFECTS ON CLUSTER GALAXIES

Fleck and Kuhn (2003-henceforth FK) argued that many of the Local Group dSph galaxies have been strongly affected by the time variable MW tide. When the internal dSph gravitational timescale is comparable to the dSph-MW orbit period important resonance effects are likely. The tide force parametrically excites the dSph and the Mathieu equation describing this interaction exhibits secular growing solutions under a broad range of orbit and galaxy density conditions. This is a feature of parametric oscillations, because resonance is strongly dependent on the amplitude of the tide and not simply on the commensurability of the internal and external driving force timescales. FK found that, under dSph conditions, parametric amplification can have a significant influence over a Hubble time when the MW

orbital angular frequency $\omega = \sqrt{\frac{GM(r)}{r^3}}$ is within a factor of about 3 of the fundamental gravitational frequency of the stellar system, $\omega_0 = \pi\sqrt{G\rho}$ where $M(r)$ is the enclosed MW mass at radius r . This condition is satisfied by some of the local dSph and FK argued that it generally accounts for their ellipticities, velocity dispersions, and extended extratidal stellar populations.

Our SDSS sample includes a large range of elliptical galaxy densities and cluster masses, but it is illustrative to note that a "typical" SDSS elliptical and galaxy cluster tend to satisfy the parametric resonance conditions. Padmanabhan et al. (2003) used SDSS data to generate elliptical galaxy mass models. Their Figure 2 "typical" SDSS mass model leads to a pulsational frequency of $\omega_0 = 2\pi/T$ with $T=30$ Myr. Cluster mass models based on x-ray and galaxy velocity dispersion constraints (e.g. Waxman and Miralda-Escude 1995) imply cluster masses of about $10^{14} M_\odot$ at a central distance of 100kpc. This leads to a circular orbit period of 75 Myr which is within

a factor of 2.5 of the galaxy internal timescale. The range in elliptical galaxy masses in these SDSS clusters is typically two orders of magnitude, and the range in cluster masses is similarly large. Thus, our sample includes clusters and member galaxies with a range of pulsational and orbital periods which broadly encompass parametric resonance conditions.

The importance of the FK mechanism is that it increases the likelihood of tidal interaction between the cluster gravitational field and its constituent galaxies. This can have three important effects: 1) it can create elliptical galaxies within the cluster, 2) it can generate intracluster light by stripping stars from the galaxies, and 3) it tends to align the affected galaxies with respect to the cluster center. Equation (25) in FK describes how galaxies in nearly circular orbits tend to have stars tidally accelerated away from their cores along a line that makes an angle θ with the direction to the cluster center. Here $\tan\theta \approx -(1 + \frac{\omega e}{2(\omega_0 - \omega)})$ and following FK, e is a dimensionless parameter that expresses the strength of the cluster gravitational tide. Galaxies affected by this mechanism will tend to be elliptical and oriented along this direction. This equation for θ shows that as a galaxy orbits in the cluster potential it will be elongated along an angle that is greater (less) than 45° to the cluster center direction, depending on whether ω_0 is greater (less) than ω . In our analysis below we compute an alignment parameter $a = (n_+ - n_-)/(n_+ + n_-)$, which is the fractional difference in number of galaxies with their long axis oriented less than (n_+) and greater than (n_-) 45° from the cluster center direction.

Over time the effect of the parametric resonance is to decrease the galaxy density, so that if ω_0 and ω were at any time of comparable magnitude then ω_0 would evolve toward *smaller* values as stars are dynamically extracted from the galaxy core. While there will also be a tendency to circularize the galaxy's orbit as energy goes toward heating the stellar system, the change in the orbital ω is smaller than the density effect on ω_0 and it eventually becomes *less* than ω even if it was initially larger. This means that those galaxies affected by the FK effect in old clusters will tend to be aligned along the radial direction (having $\theta < 45^\circ$). FK also showed numerically that non-circular orbits exhibit the same behavior, as they lead to rotating elliptical galaxies with a time averaged preference for the galaxy to be radially aligned (cf. FK – Fig. 13). Thus, in clusters that are at least several crossing times old we expect $a > 0$.

It is interesting that a numerical model of cluster galaxies (Muccione and Ciotti 2004) has found that under some conditions 10% or more of the total galaxy mass can be extracted into the intracluster environment over a Hubble time through what they call “collisionless stellar evaporation”. Because they were simulating galaxies with stellar crossing times comparable to cluster orbital periods, it is likely that they are also seeing this aspect of the parametric tidal mechanism.

We lack sufficiently detailed cluster galaxy orbit and central density information to predict how any given elliptical galaxy should be aligned. On the other hand we expect a statistical tendency toward an intrinsic radial alignment of cluster galaxies. In general this effect can be masked by non-isotropic initial conditions and a

possibly large cluster population of galaxies that do not satisfy the FK resonance conditions. Nevertheless, with a big enough galaxy and cluster sample we show here that it is possible to detect this effect.

3. A LARGE SAMPLE OF CLUSTER GALAXIES

3.1. Sample Definition

Our data is selected using the largest x-ray and optical cluster samples currently available, the Extended Brightest Clusters Sample (eBCS, Ebeling et al., 1998, 2000) and the SDSS. We obtain our cluster targets from the eBCS, a 90% complete, X-ray flux-limited sample of the brightest clusters in the northern hemisphere, compiled from the ROSAT All-Sky Survey (RASS) data. By limiting our cluster sample to known X-ray luminous clusters we avoid spurious cluster identifications from projection effects and ensure that we are looking at fairly massive systems. We crosscorrelate the eBCS list with the SDSS sky “footprint” from data release 3 (Abazajian et al. 2005). We find that out of 301 clusters, 108 are contained in the third SDSS data release.

Since the accuracy of the cluster center positions is important to this analysis, we searched the Chandra and ROSAT (HRI and PSPC) archives for pointed observations of these clusters. With much longer exposure times and better instrument resolution, the x-ray centroid can be determined within a few arcsec. 27 out of our final sample of 70 clusters have publicly available pointed data, which we adaptively smooth using the ASMOOTH code of Ebeling et al (2004) to find the new centroid position of each cluster. Improved coordinates differ from RASS coordinates by as much as 3 arcmin, with an overall median of 0.6 arcmin. We adopt the improved coordinates where available and keep RASS coordinates for the subsample that has no pointed data.

3.2. Data Extraction

For the data extraction, we define a cluster region centered on the X-ray position, 2 Mpc in radius, and a background annulus between 4 and 5 Mpc distance from the same point. We assume that this is far enough for the background region to be unaffected by the presence of the cluster but, for most clusters, close enough to suffer the same sort of systematic uncertainties intrinsic to the survey, e.g. Galactic extinction. We assume throughout a flat, Λ -dominated universe, with $\Omega_0 = 0.3$, $\Omega_\Lambda = 0.7$ and $h = 0.75$. Photometric and, where available, spectroscopic data is extracted for all galaxies (as defined by the *galaxy view* in the SDSS database) that fall within these regions and for which position angles have been determined.

3.3. Cluster Membership

The most practical and accurate way to determine which objects are gravitationally bound to the cluster is to get 3D information directly from spectroscopically determined redshifts. Any object with a redshift determined to be within $\approx 3\sigma$ of the velocity dispersion of the cluster, that is also within 2 Mpc projected distance of its center, is selected as a cluster member. We use a robust statistical estimator (ROSTAT) to derive the cluster redshift and dispersion (Beers et al., 1990). A background sample is determined from all galaxies within the

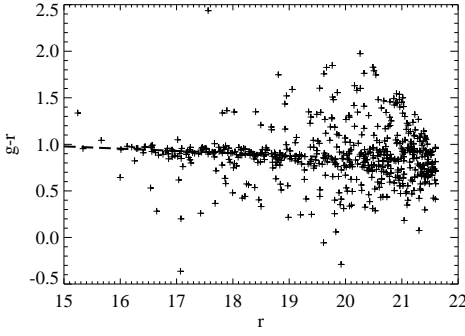


FIG. 1.— Sample galaxy cluster color magnitude diagram (cmd) with fitted red sequence as described in section 3.3

background region for each cluster. Even though limited in size, this sample is generated by an almost error-free cluster membership selection process.

In order to increase our sample size we resort to a less accurate, photometric, membership selection. Color-magnitude diagrams (CMDs) for galaxies in cluster fields allow cluster membership to be assessed based on galaxy colors. Figure 1 shows the CMD for one of the clusters analysed in this paper (Abell 2029). The dashed line indicates the best fit to the red sequence, a prominent feature of massive clusters. The red sequence is a consequence of the D_{4000} break - a characteristic of elliptical galaxies composed of old stellar populations - and the fact that galaxies in clusters are predominantly of elliptical type. By choosing filters which straddle this break at the redshift of the cluster, cluster elliptical galaxies are mostly confined to a narrow, approximately horizontal, strip in the color-magnitude diagram for these filters, i.e. the red sequence. The colors of these galaxies in these filters are very nearly the same, with a slight dependence on absolute magnitude, which gives each red sequence a characteristic slope. By examining the CMDs for each cluster, we can select elliptical cluster members by extracting only galaxies that fall within this red sequence.

We use a general, semi-automatic procedure for delimiting the red sequence boundaries in order to minimize observer bias. We use the G-R color throughout, as these are the filters that best straddle the 4000 \AA break within the redshift range of our sample. For each cluster, the three brightest objects in the CMD are located in an SDSS image of the cluster. Having correctly identified the BCGs, the median of their colors is then used as the bright end of a linear fit to all objects which fall within a horizontal box, 4 magnitudes in length from the second BCG and with a fixed color width of 0.3. We estimate the width of the red sequence by fitting a Gaussian to the dispersion of the data points around the G-R value of the best linear fit, and select all galaxies falling within $\pm 1\sigma$ of the red sequence.

Having analysed the data for the full sample we find that it is impossible to discern a well defined red sequence for some of the clusters, and are thus forced to redefine our sample. We impose an upper redshift limit ($z = 0.2$) above which cluster galaxies become too faint, and there is heavy contamination by field foreground objects, and a lower redshift limit ($z = 0.0275$) caused by the large an-

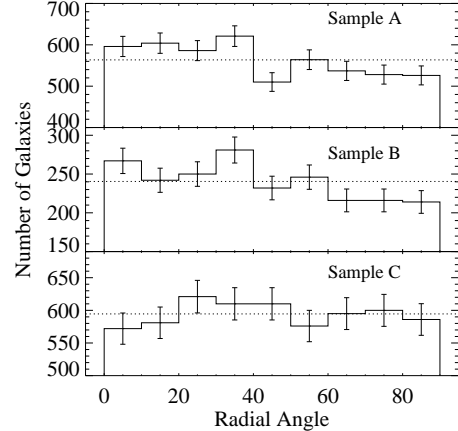


FIG. 2.— Galaxy alignment distribution for samples A,B and C. Here 0° corresponds to radial alignment of the galaxy long axis toward the cluster center. Error bars assume poisson statistics and dashed lines show the expected distribution of a 3-dimensional isotropic sample

gular size of nearby clusters and the consequent increase in contamination. A lower X-ray luminosity cutoff is also applied at $0.4 \times 10^{44} \text{ ergs s}^{-1}$, excluding clusters which are too poor to have an obvious red sequence with the available data. Hence, out of 108 clusters, 70 were included in our final analysis.

4. ALIGNMENT RESULTS

If there were no alignment tendency in our clusters the measured alignment parameters a should be consistent with zero. We determine a for each cluster and obtain its one-sigma statistical uncertainty from $\sigma_a = 1/\sqrt{n_+ + n_-}$. A weighted average over all clusters then yields the sample estimate for a . In fact we find that the largest galaxy sample (sample A - 5072 galaxies) of 70 clusters selected by redshift and CMD red-sequence membership, yields $a = 0.051 \pm 0.014$. A smaller, but potentially less background/foreground galaxy contaminated sample was obtained only from redshifts (sample B - 2133 galaxies), and yields $a = 0.072 \pm 0.021$. In contrast the sample of background galaxies from around each cluster (sample C - 5351 galaxies) yields $a = 0.005 \pm 0.014$ - consistent with zero. The alignment parameter from A and B samples are consistent, and larger than zero by 3.4σ or more. Referenced to the null hypothesis the probability of this occurring by chance is less than 3×10^{-4} . Alternatively, we present in Figure 2 a histogram of all the galaxies in samples A, B and C. The non-parametric Kolmogorov-Smirnov test is another useful check on the significance of this effect. We perform a one-sided K-S test against the null hypothesis of an isotropic 3-dimensional distribution for the alignment angle. Once again we find strong evidence that galaxies are radially aligned with a statistical significance corresponding to a 3.8σ deviation from isotropy for sample A. Sample C galaxies are, as expected, consistent with 3-dimensional galaxy orientation isotropy.

It is possible that the strength of the alignment effect varies with individual cluster properties. For example, cluster mass or age correlations are plausible, given the dependence of the parametric tide force on the cluster

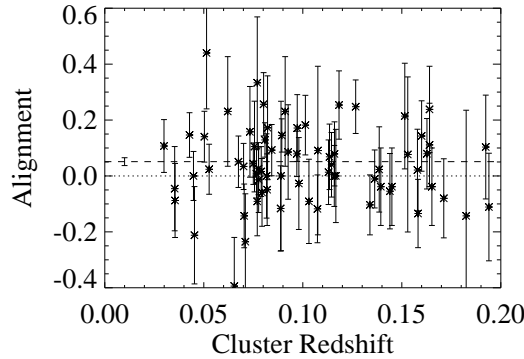


FIG. 3.— The measured alignment parameter a for the CMD-redshift-corrected sample A is plotted here versus cluster redshift. The dashed line shows the sample alignment and its one-sigma error (at $z=0.1$) and the dotted line shows the expected alignment signal for an isotropic galaxy distribution

gravitational potential and member galaxy orbits. To look for a correlation with morphology, we also used a combination of x-ray and optical images to separate clusters into 3 morphology bins, ranging from extremely relaxed systems to bimodal, heavily substructured clusters. We found no statistically significant correlation between alignment, and morphology or redshift. This is perhaps not unexpected given the statistical errors in our sample. To see this we plot all of our sample A clusters versus redshift in Figure 3. The dashed line shows the best-estimate sample alignment parameter and its 1σ error. We find that the reduced chi-squared statistic, $\chi^2_r = 0.93$, describes a cluster sample that is characterized by a single value of a and which is quite consistent with our weighted mean cluster alignment error estimates. Consequently, further investigation into possible correlations of the alignment effect with individual cluster properties will likely require a larger and/or deeper data sample.

4.1. Systematics

We are not aware of a systematic effect that can yield a fictitious radial alignment tendency in samples A and B, without affecting the control sample, C. Nevertheless, we delve briefly here into three most obvious sources of error. The impact of uncertainties in the position of the cluster centers can be assessed by comparing the results obtained using RASS coordinates and coordinates from pointed observations for the sample of 27 clusters where these

observations are available. We do not find any significant variation in the radial angle distribution and conclude that the alignment effect is robust to small uncertainties in the cluster center determination.

The second source of error is in the SDSS determination of the position angles of each galaxy. The SDSS does not provide an error estimate on this quantity so, in order to assess its significance, we look at another parameter, the gradient of the position angle with isophotal radius and its dependence on the galaxy's magnitude. We find that, at a magnitude of ≈ 19.5 , the variance in this value increases suddenly by a factor of 2. Consequently this is our cut-off for the red sequence, since extracting fainter objects only adds noise to our measurement.

The third possible source of error comes from the intrinsic uncertainties attached to the CMD method for cluster membership determination. For low redshift clusters, the faint end of the red sequence suffers contamination from background field objects, which are intrinsically fainter than cluster objects and have larger apparent magnitudes. This is evident in our data analysis, where a more significant signal (4.2σ from K-S test) is obtained when an upper limit of 17.5 magnitudes is imposed. For high redshift clusters, bright foreground field galaxies can contaminate the red sequence even at bright magnitudes. However, this alone cannot be the cause of the anisotropy observed since the effect is also present in sample B.

5. DISCUSSION

Cluster galaxies appear to show a significant tendency toward radial alignment. While there may be variations in the strength of the alignment in different clusters, to our measurement sensitivity, it appears to be a uniform and robust feature of the 70 x-ray selected clusters we studied using the SDSS dataset. We suggest that this results from the parametric tidal interaction of galaxies with their cluster gravitational potential. With a more sensitive study of galaxy alignment correlations with projected orbit, galaxy type, and cluster morphology, we look forward to using alignment as a tool to probe, and perhaps distinguish between possible mechanisms behind elliptical galaxy and cluster formation and evolution.

We thank Harald Ebeling for helpful advice on the eBCS, X-ray data analysis, and morphology classifications.

REFERENCES

Abazajian, K. and the SDSS collaboration, 2005, AJ (in press).
 Abell, G.O., Corwin, H.G., Jr., Olowin, R.P., 1989, ApJS, 70, 1
 Beers T.C., Flynn K., Gebhardt K. 1990, AJ, 100, 32
 Bingelli, B. 1982, Astron. Astrophys., 107, 338
 Brown, F.G. 1938, MNRAS, 98, 218
 Djorgovski, S. 1983, ApJ, 274, L7
 Ebeling, H., Edge, A. C., Boehringer, H., Allen, S. W., Crawford, C. S., Fabian, A. C., Voges, W., & Huchra, J. P. 1998, MNRAS, 301, 881
 Ebeling, H., Edge, A. C., Allen, S. W., Crawford, C. S., Fabian, A. C., & Huchra, J. P. 2000, MNRAS, 318, 333
 Fleck, J-J, Kuhn, J.R. 2003, ApJ, 592, 147 (FK)
 Fong, R., Stevenson, P.R.F. and Shanks, T., 1990, MNRAS, 242, 146
 Hawley, D.L., Peebles, P.J.E. 1975, AJ, 80, 477
 Kindl, E. 1987, AJ, 93, 1024
 Lambas, D., Groth, E.J., Peebles, P.J.E., 1988, AJ, 95, 975
 Moore, B., Katz, N., Lake, G., Dressler, A., Oemler, A. 1996, Nature, 379, 613
 Muccione, V. and Ciotti, L. 2004, Astron. Astrophys., 421, 583
 Plionis, M., Benoist, C., Maurogordato, S., Ferrari, C., and Basilakos, S., 2003, ApJ, 594, 144
 Thompson, L.A. 1976, ApJ, 209, 22
 Trevese, D., Cirimele, G. and Flin, P. 1992, AJ, 104, 935
 van Kampen, E., Rhee, G.F.R. 1990, Astron. Astrophys., 237, 283
 Waxman, E., Miralda-Escude, J. 1995 ApJ, 451, 451